Published in final edited form as:
Exp Cell Res. 2015 January 15; 330(2): 412–422. doi:10.1016/j.yexcr.2014.08.014.

Celastrol induces unfolded protein response-dependent cell death in head and neck cancer

Andrew M. Fribley[a,b,d,*], **Justin R. Miller**[a,d], **Amy L. Brownell**[a,d], **Danielle M. Garshott**[a,b], **Qinghua Zeng**[a,b,d], **Tyler E. Reist**[c], **Neha Narula**[d], **Peter Cai**[d], **Yue Xi**[a,d], **Michael U. Callaghan**[a,d], **Vamsi Kodali**[e], and **Randal J. Kaufman**[e,**]

[a]Carmen and Ann Adams Department of Pediatrics, Children's Hospital of Michigan, Detroit, MI 48201, USA

[b]Molecular Therapeutics Program, Barbara Ann Karmanos Cancer Institute, Detroit, MI 48201, USA

[c]The Undergraduate Research Opportunities Program, University of Michigan, Ann Arbor, MI 48109, USA

[d]Wayne State University School of Medicine, Detroit, MI, USA

[e]Degenerative Disease Research Center, Sanford|Burnham Medical Research Institute La Jolla, CA 92037, USA

Abstract

The survival rate for patients with oral squamous cell carcinoma (OSCC) has not seen marked improvement in recent decades despite enhanced efforts in prevention and the introduction of novel therapies. We have reported that pharmacological exacerbation of the unfolded protein response (UPR) is an effective approach to killing OSCC cells. The UPR is executed via distinct signaling cascades whereby an initial attempt to restore folding homeostasis in the endoplasmic reticulum during stress is complemented by an apoptotic response if the defect cannot be resolved. To identify novel small molecules able to overwhelm the adaptive capacity of the UPR in OSCC cells, we engineered a complementary cell-based assay to screen a broad spectrum of chemical matter. Stably transfected CHO-K1 cells that individually report (luciferase) on the PERK/eIF2α/ATF4/CHOP (apoptotic) or the IRE1/XBP1 (adaptive) UPR pathways, were engineered [1]. The triterpenoids dihydrocelastrol and celastrol were identified as potent inducers of UPR signaling and cell death in a primary screen and confirmed in a panel of OSCC cells and other cancer cell lines. Biochemical and genetic assays using OSCC cells and modified murine embryonic fibroblasts demonstrated that intact PERK-eIF2–ATF4-CHOP signaling is required for pro-apoptotic UPR and OSCC death following celastrol treatment.

[*]Corresponding author at: Department of Pediatrics, Children's Hospital of Michigan, 421 E. Canfield, Detroit, Michigan 48201, USA. afribley@med.wayne.edu (A.M. Fribley). [**]Corresponding author at: Sanford|Burnham Medical Research Institute, 10901 N. Torrey Pines Road, La Jolla, CA 92037, USA. rkaufman@sanfordburnham.org.

Keywords

Celastrol; ER stress; Unfolded protein response; Oral cancer; Apoptosis; Drug discovery; Chaperone; Protein folding

Introduction

A remarkable incidence of oral squamous cell carcinoma (OSCC) persists in the United States. Progress in durable patient responses has been only incremental since the introduction of cisplatin in 1978, and approximately 40,000 Americans will be newly diagnosed with oral cavity and oropharyngeal cancer this year [2]. In an attempt to improve the outcomes of conventional chemotherapy we have utilized a cell-based high throughput screening technique to identify novel small molecules that intensify the unfolded protein response (UPR) and selectively kill malignant cells [1].

The unfolded protein response (UPR) is a cell's rejoinder to the accumulation of misfolded protein in the lumen of the endoplasmic reticulum (ER). Innositol-requiring enzyme 1 alpha (IRE1α), activating transcription factor 6 (ATF6), and protein kinase RNA-like endoplasmic reticulum kinase (PERK) are three ER transmembrane sensors that continuously monitor the status of luminal protein folding. Broadly, the UPR consists of genetically distinct pathways that are simultaneously activated to either adapt to a folding challenge or initiate cell death when a stress is particularly robust or protracted. The adaptive response is directed primarily through the un-conventional splicing of a 26 base intron from X-box binding protein (*XBP*1) mRNA by IRE1α Spliced *XBP*1 yields a potent transcription factor that increases the expression of foldases, chaperones and other heat shock factors and glucose-related proteins that return to the ER in an attempt to remedy the folding defect. Although the precise mechanism governing the switch from UPR-mediated adaptation toward cell death remains an incomplete story, it is clear, when the adaptive response becomes overwhelmed, that the activation of the PERK-eIF2α-axis induces *ATF*4 and *CHOP* expression prior to apoptosis [3].

Given the rapid growth rate and highly secretory nature of many solid and hematological tumors it is not surprising that many human cancers are characterized by increased expression of translation factors and high basal levels of UPR signaling and stress. Recent studies have revealed increased expression of eukaryotic initiation factors (eIFs) and UPR-related chaperones in breast [4,5], bladder [6], lung [7], thyroid [8], lymphoma [9], colorectal [10], leukemia [11], larynx [12,13] and OSCC [11,14,15]. As malignant cell populations begin to grow and invade host tissue the extracellular tumor milieu becomes increasingly starved of oxygen, glucose and other nutrients as the rate of expansion outpaces the capacity of its vasculature. The cellular stress caused by these harsh conditions leads to IRE1α- and PERK (ATF4) -mediated angiogenesis and cell survival [16]. Importantly, Xbp1−/− fibroblasts and *Xbp*1 knockdown cells failed to form tumors in mice [17], and PERK −/− cells and xenografts are unable to tolerate hypoxia [18]. When considered together, the increased expression of translation factors and the demand for UPR-driven

angiogenesis in the tumor stroma strongly support the hypothesis that targeting the UPR with small molecules will be a productive therapeutic approach.

A cell-based high throughput screen was engineered using CHO cells transfected with luciferase reporters to specifically monitor *XBP*1 splicing or *CHOP* promoter activation [1]. A library of approximately 66,000 compounds was screened at the University of Michigan Center for Chemical Genomics and celastrol, a triterpenoid compound isolated from the plant family Celas-traceae [19], emerged as a hit that could activate both UPR reporters.

Although most studies have focused on the anti-inflammatory properties of celastrol, there are a growing number of reports highlighting its use as a promising anti-cancer compound in breast leukemia, melanoma, myeloma, pancreatic and prostate cell culture and xenograft models [20–24]. The anti-proliferative effects of celastrol have been attributed to mechanisms involving diverse signaling networks that include the inhibition of pro-survival NF-B signaling, proteasome inhibition and the up-regulation of pro-apoptotic Bcl-2 family members and down regulation of anti-apoptotic genes such as Bcl-2 and XIAP. Since celastrol has been shown to potently induce the expression of heat shock proteins [25] and was able to activate UPR luciferase reporters in our screen, we hypothesized that its ability to induce cell death and reduce xenograft tumor burden in several models might be dependent on its ability to activate the UPR.

Experimental procedures

Cell lines, reporters and reagents

Stably transfected CHO-K1 cells containing pathway-specific luciferase reporters for the PERK/eIF2α/CHOP pathway or the IRE1/XBP1 pathway were used for screening as described [1]. The human floor of mouth squamous cell carcinoma lines UMSCC1, UMSCC14A and laryngeal squamous cell carcinoma cell line UMSCC23 were kindly provided by Dr. Thomas Carey at the University of Michigan. The tongue carcinoma cell line CAL27 (CRL-2095), the salivary epidermoid carcinoma cell line A-253 (HTB-41) and the pharyngeal carcinoma cell line FaDu (HTB-43) were from ATCC (Manassas, VA). A549 BAX−/−/−/−, BAK−/− lung adenocarcinoma cells (CLLS1015) were from Sigma. All human cancer cell lines were cultured in DMEM supplemented with penicillin and streptomycin and 10% fetal bovine serum. Normal human epidermal keratinocytes (nHEK), associated medium, culture reagents and supplements were from Science Cell Research Laboratories (Carlsbad, CA). Celastrol was purchased from Enzo Life Sciences (San Diego, CA) and dihydrocelastrol was from Microsource Discovery Systems Inc. (Gaylordsville, CT).

PCR—Quantitative real time reverse-transcription PCR (RT-qPCR) and conventional reverse-transcription PCR (RT-PCR) were performed with cDNA prepared with Cells to CT™ (Life Technologies, Carlsbad, CA), as described [26]. Semi-quantitative RT-PCR analysis of spliced and un-spliced *XBP*1 was performed with a single human-specific primer pair ACA CGC TTG GGA ATG GAC AC (forward) and CCA TGG GAA GAT GTT CTG GG (reverse) [27]; amplicons were visualized with a Qiagen Qiaxcel automated nucleic acid fragment analyzer using a high resolution cartridge on the M500 setting using a 15 bp–1 kb

alignment marker and a 50 bp–800 bp size marker. qRT-PCR was performed with following Taqman primer/probe sets: CHOP/DDIT3 (Hs01090850_m1), 18S (Hs99999901_s1), GADD34 (Hs00169585_ m1), ATF3 (Hs00910173_m1), ATF4 (Hs00909569_g1), BiP/GRP78 (Hs99999174_m1), HERPUD1 (Hs00206652_m1), DR5 (Hs00366278_ m1), TRB3 (Hs00221754_m1), ERDJ4 (Hs00202448_m1), ERDJ5 (Hs00943467_m1), EDEM (Hs00976004_m1), $p21^{WAF}$ (Hs00355782_ m1), XBP1 (spliced) (Hs03929085_g1), Bim (Hs00708019_s1), Bid (Hs00609632_m1), NOXA (Hs00560402_m1), PUMA (Hs00248075_ m1) and NBK (Hs00154189_m1). All experiments were performed at least three times; representative experiments depict technical replicates also performed in triplicate.

Viability and caspase assays

Trypan blue-exclusion assay or the luminescent Cell Titer-Glo Cell Viability Assay (G7570) (Promega Corp., Madison, WI) were used. Caspase activation was measured with a luminescent Caspase-Glo 3/7 Assay (Promega, Madison, WI). For luminescent assays 12,500 cells were seeded in 96 well white culture plates. Concentrations of celastrol above 5 μM appeared to enhance luciferase activity and consistently provided false-positive proliferation data as validated with trypan blue exclusion assays (data not shown). For colony formation assay, 1000 cells were plated in 6 cm tissue culture dishes and exposed to celastrol for 1 h. Cultures were maintained until vehicle (DMSO) treated colonies reached 50 cells. Cultures were washed, fixed with methanol and stained with bromophenol blue. The number of 50 cell colonies in celastrol treated wells were counted and reported as a percentage of the vehicle treated cells.

Western blot analysis

Whole-cell lysates were prepared in modified RIPA buffer with PMSF and protease inhibitors. 25–50 μg of lysate was resolved on 8 or 12% SDS-PAGE gels and transferred to PVDF membrane (Bio-Rad, Hercules, CA). Antibodies were from the following sources: Caspases 3 and 9, Cell Signaling (Beverly, MA); ATF-4, BAK, CHOP, and ubiquitin Santa Cruz (Santa Cruz, CA); GAPDH, Millipore (Billerica, MA)

Statistics—Statistic analyses were performed using Microsoft Excel 2013 (Redmond, WA) and consisted of descriptive statistics (means and standard deviations). Comparative tests included *t*-tests and 2 way ANOVA performed with GraphPad Prism version 6 for Mac (La Jolla, CA). All *P*-values are two-sided. *P*-values lower than 0.05 were considered statistically significant.

Results

Celastrol activates the unfolded protein response

The tripterine celastrol emerged as a hit in a high throughput screen to identify small molecule activators of the unfolded protein response (UPR). Confirmatory dose-response assays demonstrated activation of the CHOP- and XBP1-luciferase reporters used in the primary screen [1,28] (Fig. 1A). The closely related analog dihydrocelastrol was active only at substantially higher concentrations (data not shown). A panel of oral squamous cell

carcinoma (OSCC) cell lines exposed to celastrol displayed increased levels of UPR-related mRNA transcripts (Fig. 1B) and *XBP*1 splicing (Fig. 1C), confirming its ability to induce ER stress and activate the UPR. In general, higher concentrations of celastrol were required to activate UPR gene expression and *XBP*1 splicing in FaDu cells, which are known to harbor a SMAD4/TGFβR signaling defect. Celastrol has been reported to inhibit the chymotrypsin-like activity of the 26S proteasome in prostate cancer [29] and rat glioma cells [30], another well-characterized mechanism of UPR induction by our group and others [31–33]. Fluorescent (Z-gly-gly-leu-AMC) 26S proteasome assay could detect only very modest reductions in proteasome function in UMSCC14A and UMSCC23 cells after 1, 3 or 6 h, and only at concentrations well above the observed IC50 values of celastrol (Fig. 1D). These data were confirmed in a concentration and time course study using a luminescent 26S chymotrypsin-like assay in UMSCC1 cell cultures (data not shown). Considered together, these data indicate that celastrol induces proteasome-inhibition-independent ER stress and the UPR in OSCC cells.

Celastrol inhibits proliferation of oral squamous cell carcinoma (OSCC) cells and increases apoptosis-related transcripts

ATP-based luminescent proliferation assays indicated that celastrol could potently inhibit growth in a panel of OSCC cell lines (Fig. 2A); significantly higher concentrations were again required to observe an effect in dihydrocelastrol treated cultures (data not shown). OSCC cell lines with known SMAD4/TGFβR signaling defects displayed 2–7 fold higher IC50 values than cell lines with intact SMAD4/TGFβR signaling (Fig. 2B). Concentration- and time-dependent experiments with normal human epidermal keratinocytes revealed an IC50 of ~4.0 μM at 16 and 24 h (Fig. 2C), indicating a 5+ fold decrease in sensitivity compared to the OSCC cell lines with intact SMAD4/TGFβR signaling. Clonogenic survival assays to measure the long-term cytostatic/cytotoxic effects of celastrol revealed that<1.0 μM celastrol for one hour (prior to washout) could inhibit the ability of ≥50% of cultures to grow to 50-cell colonies after 10–14 days, compared to DMSO (vehicle) controls (Fig. 2D). RT-qPCR interrogation of cDNA's generated from celastrol treated UMSCC1, UMSCC14A and FaDu cells demonstrated increased mRNA transcripts of the apoptotic BH3-only BCL2 family members *NOXA* and *PUMA* and for the UPR-associated death genes *TRB*3 and *GADD*45*β* (Fig. 2E). The observation that *NOXA* and *PUMA* transcripts were only slightly induced in the resistant FaDu cells suggests that the accumulation of BH3-only family members might be required for celastrol to modulate cancer cell proliferation and cell death. Celastrol IC50 values for the neuroblastoma cell lines SH-SY5Y and SH-BE were similar to OSCC cells with intact TGFβR/SMAD4 (data not shown), indicating that the ability of celastrol to inhibit cancer cell proliferation is not a phenomenon unique to OSCC.

Celastrol leads to increased accumulation of polyubiquitinated proteins and apoptosis in OSCC

Having observed increased apoptosis-related mRNA transcripts we sought to determine the extent to which programed cell death might be governing the ability of celastrol to reduce proliferation. Luminescent Caspase3/7 assays revealed increased enzyme activity by eight hours in UMSCC1 but not celastrol-resistant FaDu cells, even at a ten-fold higher concentration (Fig. 3A). Immunoblot analysis of whole cell lysates further demonstrated

celastrol treatment reduced the pro-form of caspase 9 and led to the accumulation of active caspase 3 (Fig. 3B), consistent with the observations of others [34–36]. Increased accumulation of pro-apoptotic BAK was also observed following celastrol treatment (Fig. 3C), a finding that has not been previously reported. Neither caspase activation nor BAK accumulation was evident in celastrol-resistant FaDu cells. (Fig. 3B and C). Human DLD1 colorectal adenocarcinoma cells doubly deficient for BAX and BAK were significantly resistant to celastrol (Fig. 3D); and electrophoretic resolution of genomic DNA from celastrol treated cells revealed laddering only in celastrol-sensitive OSCC cell lines (Fig. 3E). These data confirm a role for the intrinsic (mitochondrial) apoptotic pathway in celastrol-mediated cancer cell death and extend previous observations that it can induce apoptosis in cultured cells [29,34,37]. The ability of celastrol to induce ubiquitination (Ub) in whole cell lysates has been reported in different cancer subtypes [20,36,37]. Immunoblot analysis revealed that celastrol-resistant cell lines (CAL27 and FaDu) accumulated Ub proteins much more slowly than celastrol-sensitive UMSCC23 cells (Fig. 3F). These data indicated that apoptosis is a key feature in celastrol-mediated reductions in OSCC proliferation, and suggested that reduced accumulation of Ub proteins might be a feature of celastrol-resistance.

The ability of celastrol to induce apoptosis is UPR-dependent

Cultures of murine embryonic fibroblasts (MEF) bearing mutations in key UPR genes were employed to study the link between celastrol-mediated apoptosis and the UPR. Trypan blue-exclusion assays demonstrated *eIF2α* Ser51Ala mutant (A/A) MEF experienced greater cell death than wildtype (S/S) littermate controls, a key feature of ER stress-inducing compounds [38]. After 6 h exposure to increasing concentrations of celastrol A/A MEF's displayed only trace accumulation of Atf4, no Chop, and a pronounced decrease of pro-caspase 9 and increased cleaved caspase 3 (Fig. 4A). A/A cells accumulated Ub proteins much more rapidly than the more resistant S/S cells (Fig. 4A). *Atf*4-null MEF's were significantly resistant to celastrol, demonstrated only modest accumulation of Chop and the apoptotic fragments of caspases 9 and 3 and displayed fewer Ub proteins, that wildtype (Fig. 4B). Experiments with paired *Chop*-null and wildtype MEF indicated intact *Chop* signaling was necessary for efficient celastrol-mediated cell killing and accumulation of Atf4 was the same in wildtype and Chop null cells (Fig. 4C). However, immunoblot analysis unexpectedly revealed the kinetics of caspase 9 and −3 activation to be very similar. We hypothesized this result was reflective of the narrow window where the significant difference between the two cell lines became apparent in 6 h dose-response analysis (i.e. only at 1.25 μM). An enzymatic caspase 3/7 assay demonstrated significantly more caspase activity in wildtype MEF at four and 8 h in a dose-dependent fashion (Fig. 4D). Considered together, these data indicate that the ability of celastrol to induce apoptosis is impaired in MEF with UPR mutations downstream of *eIF2α* and that increased ubiquitination is a feature of celastrol-sensitive MEF.

Discussion

The recent surge of publications delineating molecular mechanisms by which natural products act as anticancer agents is reflective of a world-wide desire to identify novel cost-

effective therapies from the biota. Many natural products including celastrol have been used in traditional culture-specific medical practices for hundreds of years and offer tremendous promise in that their ability to be administered and tolerated in humans is largely known. Celastrol is derived from *Tripteryguim wilfordii* and is recognized to have potent anti-inflammatory and anticancer properties [39]. A high throughput screen of small molecules and natural extracts identified the ability of celastrol and its close analog dihydrocelastrol to activate the UPR. The present study demonstrates through the use of biochemical and genetic models that celastrol induces stress in the endoplasmic reticulum (ER) and activates a terminal UPR in a panel of OSCC, other cancer cell lines and MEF.

Recently, celastrol has been studied as an anticancer agent in a variety of *in vitro* and xenograft models, and has been reported to activate the heat shock response [40], the UPR [36,41], inhibit NK-κB [15,42,43] and interfere with angiogenesis via VEGF suppression [44]. The mechanisms by which these compounds mete out their cytotoxic effects have also been well studied. Our finding that celastrol leads to accumulation of the pro-apoptotic BCL2 family member Bak, furthers previous observations that Bax and NOXA were induced in glioma [30] and prostate cancer cells [42], respectively. The death inducing effect of these transcripts is very likely bolstered by the fact that celastrol can simultaneously inhibit anti-apoptotic BCL2 and XIAP [30] prior to caspase activation. The work of many others has reported the activation of caspases -3, -8 and -9 and cleavage of PARP prior to celastrol-mediated cell death [30,35,37,42], consistent with our findings. This is the first report to the best of our knowledge however, that celastrol can induce apoptosis-related BAK, *Puma* and *Trb*3 expression prior to cell death.

The current study demonstrated that celastrol could induce the UPR, activate the intrinsic apoptosis cascade and inhibit growth in a panel of seven OSCC cell lines. It was recently reported that similar doses of celastrol led to the accumulation of the ER resident chaperone BiP/Grp78 in HeLa cells [45], and it is known that celastrol can induce CHOP [34] and *GADD*34 [46]. These data support the conclusion that ER stress might be a primary mechanism by which celastrol exerts is cytotoxic effects. Using MEF we show that an intact Perk-eIF2α-Atf4-Chop arm of the UPR is required for efficient cell death. Important mechanistic insight can be gleaned from murine fibroblasts even though they may not exactly recapitulate human cancer cell signaling. Human cancer cell models of *ATF*4 and *CHOP* knockdown/knockout using siRNA, TALENs or CRISPRs have been problematic in that the culture media require the addition of antioxidants and other supplements that confound studies with oxidative stressors such as celastrol (unpublished observation). Our study demonstrated that eIF2α Ser51Ala mutant (A/A) MEF, which cannot undergo the translational pause required to mount a productive UPR [38], experienced significantly greater caspase activation and chop-independent cell death. In cells that could undergo the protective pause in translation (i.e. express wildtype eIF2α) deletion of Atf4, which reduced Chop, or the deletion of Chop alone, was sufficient to significantly attenuate the cytotoxic effect of celastrol; see model (Fig. 5). Although these effects are likely mediated, at least in part, by Perk it is possible that more than one eIF2α kinase might be activated by celastrol. In support of this notion, it was reported that celastrol-mediated death could be prevented in breast adenocarcinoma cultures with the addition of the general ROS scavenging antioxidant

N-acetyl cysteine [34]. The superoxide-specific scavengers tempol and tiron could not provide any protection (unpublished observation). Regardless, it is possible that free radical induction by celastrol might activate other eIF2α kinases (e.g. HRI), which might serve to enhance or prolong the UPR and lead to cell death. How other eIF2α kinases might regulate celastrol-induced cell death was not the focus of the current study and is not currently clear.

Although reliable reports have indicated that concentrations of celastrol similar to those used in the current study could inhibit the chymotrypsin-like activity of the 26S proteasome [37,42], a mechanism known induce the UPR, we could only detect modest inhibition (and only in one of two different assays) prior to the induction of UPR markers or death. This may be partially explained by the fact that we observed convincing UPR induction by six hours and other work analyzed proteasome activity after 12 h [37]. This group also observed an accumulation of polyubiquitinated proteins after only 4 h, consistent with other reports [36,45,47] and likely indicates an attempt by the cell to clear client peptides through ERAD. The accumulation of polyubiquitinated proteins alone is not a surrogate measure of proteasome function [47]. Our group and others have demonstrated that proteasome inhibition can induce ER stress and the UPR in a variety of cancer cell types [32,48–50]; however, celastrol does not appear to utilize this mechanism in OSCC.

Currently, there is tremendous interest in identifying the mechanism/s by which spontaneous tumors develop in *Smad*4 −/− mice and why *TGFβR*- and *SMAD4*-deficient OSCC's are particularly resistant to chemotherapy in the clinic. Our studies unexpectedly revealed that FaDu, A253 and Cal27, three OSCC cell lines known to have impaired *TGFβR*- and *SMAD*4 signaling, displayed IC50 values 3–5 times higher than cells without these defects. Although they were less sensitive to celastrol, the IC50 values were still <10 μM, suggesting the possibility of a therapeutic benefit even for tumors bearing *TGFβR* and *SMAD*4 signaling defects. Further studies with additional cell lines harboring these mutations are necessary to validate this hypothesis.

There is significant interest in the discovery and development of small molecules and natural products that modulate the UPR for a variety of human diseases where there is a paucity of treatments or none at all. In the current study we demonstrate that the natural product celastrol induces ER stress and a terminal UPR in OSCC cells. This study provides an example of the power of a productive high throughput screen to identify small molecules that target specific sub-cellular pathways involved in UPR signaling and malignancy.

Acknowledgments

This research was supported by DE019678, the Wayne State University Fund for Medical Research and the Children's Research Foundation of Michigan (A.M.F.) and DK088227, HL057346, DK0422394 (R.J.K).

References

1. Fribley AM, Cruz PG, Miller JR, Callaghan MU, Cai P, Narula N, Neubig RR, Showalter HD, Larsen SD, Kirchhoff PD, Larsen MJ, Burr DA, Schultz PJ, Jacobs RR, Tamayo-Castillo G, Ron D, Sherman DH, Kaufman RJ. Complementary cell-based high-throughput screens identify novel modulators of the unfolded protein response. J Biomol Screen. 2011; 16:825–835. [PubMed: 21844328]

2. Jemal A, Siegel R, Ward E, Hao Y, Xu J, Thun MJ. Cancer statistics, 2009. CA: Cancer J Clin. 2009; 59:225–249. [PubMed: 19474385]

3. Han J, Back SH, Hur J, Lin YH, Gildersleeve R, Shan J, Yuan CL, Krokowski D, Wang S, Hatzoglou M, Kilberg MS, Sartor MA, Kaufman RJ. ER-stress-induced transcriptional regulation increases protein synthesis leading to cell death. Nat Cell Biol. 2013; 15:481–490. [PubMed: 23624402]

4. Larsson O, Li S, Issaenko OA, Avdulov S, Peterson M, Smith K, Bitterman PB, Polunovsky VA. Eukaryotic translation initiation factor 4E induced progression of primary human mammary epithelial cells along the cancer pathway is associated with targeted translational deregulation of oncogenic drivers and inhibitors. Cancer Res. 2007; 67:6814–6824. [PubMed: 17638893]

5. Kerekatte V, Smiley K, Hu B, Smith A, Gelder F, De Benedetti A. The proto-oncogene/translation factor eIF4E: a survey of its expression in breast carcinomas. Int J Cancer. 1995; 64:27–31. [PubMed: 7665244]

6. Crew JP, Fuggle S, Bicknell R, Cranston DW, de Benedetti A, Harris AL. Eukaryotic initiation factor-4E in superficial and muscle invasive bladder cancer and its correlation with vascular endothelial growth factor expression and tumour progression. Br J Cancer. 2000; 82:161–166. [PubMed: 10638984]

7. Rosenwald IB, Hutzler MJ, Wang S, Savas L, Fraire AE. Expression of eukaryotic translation initiation factors 4E and 2alpha is increased frequently in bronchioloalveolar but not in squamous cell carcinomas of the lung. Cancer. 2001; 92:2164–2171. [PubMed: 11596034]

8. Wang S, Lloyd RV, Hutzler MJ, Rosenwald IB, Safran MS, Patwardhan NA, Khan A. Expression of eukaryotic translation initiation factors 4E and 2alpha correlates with the progression of thyroid carcinoma. Thyroid. 2001; 11:1101–1107. [PubMed: 12186496]

9. Wang S, Rosenwald IB, Hutzler MJ, Pihan GA, Savas L, Chen JJ, Woda BA. Expression of the eukaryotic translation initiation factors 4E and 2alpha in non-Hodgkin's lymphomas. Am J Pathol. 1999; 155:247–255. [PubMed: 10393856]

10. Rosenwald IB, Chen JJ, Wang S, Savas L, London IM, Pullman J. Upregulation of protein synthesis initiation factor eIF-4E is an early event during colon carcinogenesis. Oncogene. 1999; 18:2507–2517. [PubMed: 10229202]

11. Assouline S, Culjkovic B, Cocolakis E, Rousseau C, Beslu N, Amri A, Caplan S, Leber B, Roy DC, Miller WH Jr, Borden KL. Molecular targeting of the oncogene eIF4E in acute myeloid leukemia (AML): a proof-of-principle clinical trial with ribavirin. Blood. 2009; 114:257–260. [PubMed: 19433856]

12. Franklin S, Pho T, Abreo FW, Nassar R, De Benedetti A, Stucker FJ, Nathan CO. Detection of the proto-oncogene eIF4E in larynx and hypopharynx cancers. Arch Otolaryngol Head Neck Surg. 1999; 125:177–182. [PubMed: 10037284]

13. Altman BJ, Wofford JA, Zhao Y, Coloff JL, Ferguson EC, Wieman HL, Day AE, Ilkayeva O, Rathmell JC. Autophagy provides nutrients but can lead to Chop-dependent induction of Bim to sensitize growth factor-deprived cells to apoptosis. Mol Biol Cell. 2009; 20:1180–1191. [PubMed: 19109422]

14. Nathan CO, Liu L, Li BD, Abreo FW, Nandy I, De Benedetti A. Detection of the proto-oncogene eIF4E in surgical margins may predict recurrence in head and neck cancer. Oncogene. 1997; 15:579–584. [PubMed: 9247311]

15. He D, Xu Q, Yan M, Zhang P, Zhou X, Zhang Z, Duan W, Zhong L, Ye D, Chen W. The NF-kappa B inhibitor, celastrol, could enhance the anti-cancer effect of gambogic acid on oral squamous cell carcinoma. BMC Cancer. 2009; 9:343. [PubMed: 19778460]

16. Feldman DE, Chauhan V, Koong AC. The unfolded protein response: a novel component of the hypoxic stress response in tumors. Mol Cancer Res: MCR. 2005; 3:597–605.

17. Romero-Ramirez L, Cao H, Nelson D, Hammond E, Lee AH, Yoshida H, Mori K, Glimcher LH, Denko NC, Giaccia AJ, Le QT, Koong AC. XBP1 is essential for survival under hypoxic conditions and is required for tumor growth. Cancer Res. 2004; 64:5943–5947. [PubMed: 15342372]

18. Bi M, Naczki C, Koritzinsky M, Fels D, Blais J, Hu N, Harding H, Novoa I, Varia M, Raleigh J, Scheuner D, Kaufman RJ, Bell J, Ron D, Wouters BG, Koumenis C. ER stress-regulated

translation increases tolerance to extreme hypoxia and promotes tumor growth. EMBO J. 2005; 24:3470–3481. [PubMed: 16148948]

19. Abbott A. Neurologists strike gold in drug screen effort. Nature. 2002; 417:109. [PubMed: 12000928]
20. Raja SM, Clubb RJ, Ortega-Cava C, Williams SH, Bailey TA, Duan L, Zhao X, Reddi AL, Nyong AM, Natarajan A, Band V, Band H. Anticancer activity of Celastrol in combination with ErbB2-targeted therapeutics for treatment of ErbB2-overexpressing breast cancers. Cancer Biol Ther. 2011; 11:263–276. [PubMed: 21088503]
21. Pang X, Yi Z, Zhang J, Lu B, Sung B, Qu W, Aggarwal BB, Liu M. Celastrol suppresses angiogenesis-mediated tumor growth through inhibition of AKT/mammalian target of rapa-mycin pathway. Cancer Res. 2010; 70:1951–1959. [PubMed: 20160026]
22. Abbas S, Bhoumik A, Dahl R, Vasile S, Krajewski S, Cosford ND, Ronai ZA. Preclinical studies of celastrol and acetyl isogambogic acid in melanoma. Clin Cancer Res Off J Am Assoc Cancer Res. 2007; 13:6769–6778.
23. Peng B, Xu L, Cao F, Wei T, Yang C, Uzan G, Zhang D. HSP90 inhibitor, celastrol, arrests human monocytic leukemia cell U937 at G0/G1 in thiol-containing agents reversible way. Mol Cancer. 2010; 9:79. [PubMed: 20398364]
24. Chen M, Rose AE, Doudican N, Osman I, Orlow SJ. Celastrol synergistically enhances temozolomide cytotoxicity in melanoma cells. Mol Cancer Res: MCR. 2009; 7:1946–1953.
25. Chow AM, Brown IR. Induction of heat shock proteins in differentiated human and rodent neurons by celastrol. Cell Stress Chaperones. 2007; 12:237–244. [PubMed: 17915556]
26. Fribley AM, Miller JR, Reist TE, Callaghan MU, Kaufman RJ. Large-Scale Analysis of UPR-Mediated Apoptosis in Human Cells. Methods Enzymol. 491:57–71. [PubMed: 21329794]
27. Park JW, Woo KJ, Lee JT, Lim JH, Lee TJ, Kim SH, Choi YH, Kwon TK. Resveratrol induces pro-apoptotic endoplasmic reticulum stress in human colon cancer cells. Oncol Rep. 2007; 18:1269–1273. [PubMed: 17914584]
28. Flaherty, DP.; Golden, JE.; Liu, C.; Hedrick, M.; Gosalia, P.; Li, Y.; Milewski, M.; Sugarman, E.; Suyama, E.; Nguyen, K.; Vasile, S.; Salaniwal, S.; Stonich, D.; Su, Y.; Mangravita-Novo, A.; Vicchiarelli, M.; Smith, LH.; Diwan, J.; Chung, TDY.; Pinkerton, AB.; Aube, J.; Miller, JR.; Garshott, DM.; Callaghan, MU.; Fribley, AM.; Kaufman, RJ. Probe Reports from the NIH Molecular Libraries Program. Bethesda (MD): 2010. Selective small molecule activator of the apoptotic arm of the UPR.
29. Yang HS, Kim JY, Lee JH, Lee BW, Park KH, Shim KH, Lee MK, Seo KI. Celastrol isolated from Tripterygium regelii induces apoptosis through both caspase-dependent and -independent pathways in human breast cancer cells. Food Chem Toxicol: Int J published Br Indus Biol Res Assoc. 2011; 49:527–532.
30. Ge P, Ji X, Ding Y, Wang X, Fu S, Meng F, Jin X, Ling F, Luo Y. Celastrol causes apoptosis and cell cycle arrest in rat glioma cells. Neurol Res. 2010; 32:94–100. [PubMed: 19909582]
31. Fribley A, Zeng Q, Wang CY. Proteasome inhibitor PS-341 induces apoptosis through induction of endoplasmic reticulum stress-reactive oxygen species in head and neck squamous cell carcinoma cells. Mol Cell Biol. 2004; 24:9695–9704. [PubMed: 15509775]
32. Bush KT, Goldberg AL, Nigam SK. Proteasome inhibition leads to a heat-shock response, induction of endoplasmic reticulum chaperones, and thermotolerance. J BiolChem. 1997; 272:9086–9092.
33. Perez-Galan P, Roue G, Villamor N, Montserrat E, Campo E, Colomer D. The proteasome inhibitor bortezomib induces apoptosis in mantle-cell lymphoma through generation of ROS and Noxa activation independent of p53 status. Blood. 2006; 107:257–264. [PubMed: 16166592]
34. Sung B, Park B, Yadav VR, Aggarwal BB. Celastrol, a triterpene, enhances TRAIL-induced apoptosis through the down-regulation of cell survival proteins and up-regulation of death receptors. J Biol Chem. 2010; 285:11498–11507. [PubMed: 20154087]
35. Sethi G, Ahn KS, Pandey MK, Aggarwal BB. Celastrol, a novel triterpene, potentiates TNF-induced apoptosis and suppresses invasion of tumor cells by inhibiting NF-kappaB-regulated gene products and TAK1-mediated NF-kappaB activation. Blood. 2007; 109:2727–2735. [PubMed: 17110449]

36. Zhu H, Yang W, He LJ, Ding WJ, Zheng L, Liao SD, Huang P, Lu W, He QJ, Yang B. Upregulating Noxa by ER stress, celastrol exerts synergistic anti-cancer activity in combination with ABT-737 in human hepatocellular carcinoma cells. PLoS One. 2012; 7:e52333. [PubMed: 23284992]
37. Yang H, Chen D, Cui QC, Yuan X, Dou QP. Celastrol, a triterpene extracted from the Chinese Thunder of God Vine, is a potent proteasome inhibitor and suppresses human prostate cancer growth in nude mice. Cancer Res. 2006; 66:4758–4765. [PubMed: 16651429]
38. Scheuner D, Song B, McEwen E, Liu C, Laybutt R, Gillespie P, Saunders T, Bonner-Weir S, Kaufman RJ. Translational control is required for the unfolded protein response and in vivo glucose homeostasis. Mol Cell. 2001; 7:1165–1176. [PubMed: 11430820]
39. Setty AR, Sigal LH. Herbal medications commonly used in the practice of rheumatology: mechanisms of action, efficacy, and side effects. Sem Arthr Rheum. 2005; 34:773–784.
40. Westerheide SD, Bosman JD, Mbadugha BN, Kawahara TL, Matsumoto G, Kim S, Gu W, Devlin JP, Silverman RB, Morimoto RI. Celastrols as inducers of the heat shock response and cytoprotection. J Biol Chem. 2004; 279:56053–56060. [PubMed: 15509580]
41. Mu TW, Ong DS, Wang YJ, Balch WE, Yates JR 3rd, Segatori L, Kelly JW. Chemical and biological approaches synergize to ameliorate protein-folding diseases. Cell. 2008; 134:769–781. [PubMed: 18775310]
42. Dai Y, Desano J, Tang W, Meng X, Meng Y, Burstein E, Lawrence TS, Xu L. Natural proteasome inhibitor celastrol suppresses androgen-independent prostate cancer progression by modulating apoptotic proteins and NF-kappaB. PLoS One. 2010; 5:e14153. [PubMed: 21170316]
43. Zhou LL, Lin ZX, Fung KP, Cheng CH, Che CT, Zhao M, Wu SH, Zuo Z. Celastrol-induced apoptosis in human HaCaT keratinocytes involves the inhibition of NF-kappaB activity. Eur J pharmacol. 2011; 670:399–408. [PubMed: 21951963]
44. Huang Y, Zhou Y, Fan Y, Zhou D. Celastrol inhibits the growth of human glioma xenografts in nude mice through suppressing VEGFR expression. Cancer Lett. 2008; 264:101–106. [PubMed: 18343027]
45. Wang WB, Feng LX, Yue QX, Wu WY, Guan SH, Jiang BH, Yang M, Liu X, Guo DA. Paraptosis accompanied by autophagy and apoptosis was induced by celastrol, a natural compound with influence on proteasome, ER stress and Hsp90. J Cell Physiol. 2011
46. Trott A, West JD, Klaic L, Westerheide SD, Silverman RB, Morimoto RI, Morano KA. Activation of heat shock and antioxidant responses by the natural product celastrol: transcriptional signatures of a thiol-targeted molecule. Mol Biol Cell. 2008; 19:1104–1112. [PubMed: 18199679]
47. Menendez-Benito V, Verhoef LG, Masucci MG, Dantuma NP. Endoplasmic reticulum stress compromises the ubiquitin-proteasome system. Human Mol Genet. 2005; 14:2787–2799. [PubMed: 16103128]
48. Fribley A, Wang CY. Proteasome inhibitor induces apoptosis through induction of endoplasmic reticulum stress. Cancer Biol Ther. 2006; 5:745–748. [PubMed: 16861900]
49. Nawrocki ST, Carew JS, Dunner K Jr, Boise LH, Chiao PJ, Huang P, Abbruzzese JL, McConkey DJ. Bortezomib inhibits PKR-like endoplasmic reticulum (ER) kinase and induces apoptosis via ER stress in human pancreatic cancer cells. Cancer Res. 2005; 65:11510–11519. [PubMed: 16357160]
50. Fels DR, Ye J, Segan AT, Kridel SJ, Spiotto M, Olson M, Koong AC, Koumenis C. Preferential cytotoxicity of bortezomib toward hypoxic tumor cells via overactivation of endoplasmic reticulum stress pathways. Cancer Res. 2008; 68:9323–9330. [PubMed: 19010906]

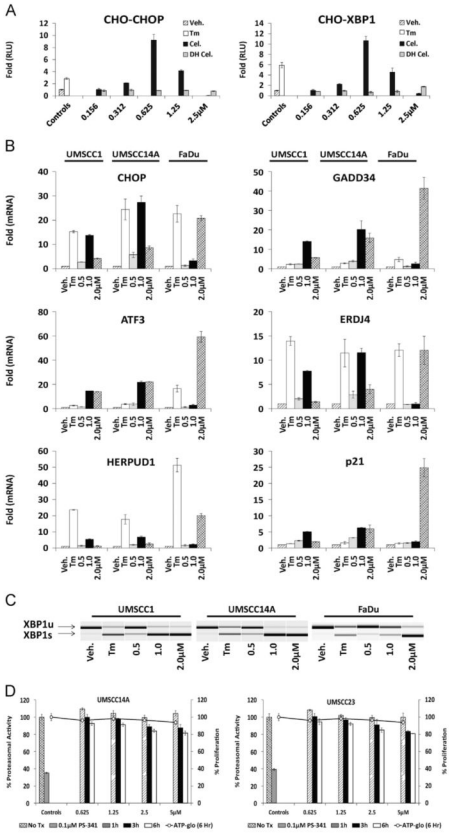

Fig. 1.

Celastrol induces unfolded protein response. A. Stable CHO-K1 cells containing UPR-luciferase reporters were treated with tunicamycin (Tm), celastrol (Cel) or dihydrocelastrol (DH Cel) for 8 h. B. RT-qPCR analysis of UPR-associated genes in a panel of OSCC treated with Tm or increasing doses of celastrol for 6 h. For RT-qPCR 18 s ribosomal RNA was used as internal control and fold changes were determined using the delta delta CT calculation; error bars represent standard deviation of technical replicates. C. cDNA was generated with the same RNA used in B (above) and conventional RT-PCR was performed with a single primer pair to appreciate relative levels of unspliced (XBP1u) and spliced (XBP1s) mRNA. D. Fluorescent (Z-gly-gly-leu-AMC) 26S proteasome assay with celastrol treated UMSCC14A and UMSCC23 cells after 1, 3 and 6 h. To control for cell death, which might artificially reduce assay signal, an ATP-based proliferation was performed on identically treated cells at for each data point on the same 96 well plate (right *Y*- axis, line graph). PS-341 (bortezomib) is a potent and selective inhibitor of the chymotrypsin-like activity of the 26S proteasome.

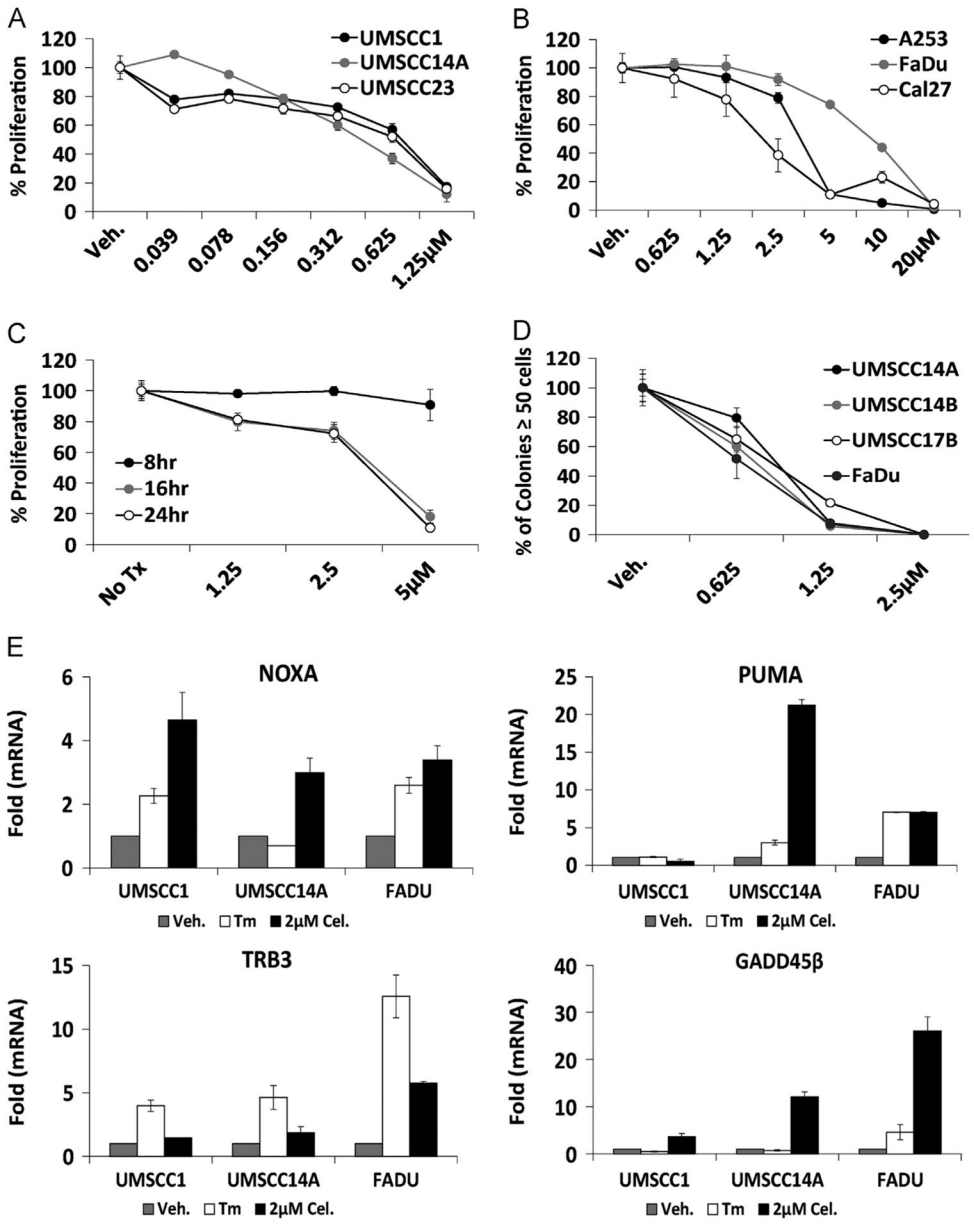

Fig. 2.

Celastrol reduces proliferation of OSCC cells and induces apoptotic mRNA transcripts. A. Luminescent ATP-based proliferation assays performed with OSCC cell lines after 24 h exposure to celastrol (IC_{50} 0.44–0.77). B. Luminescent ATP-based proliferation assays performed in TGFβ/SMAD-mutant OSCC cell lines after 24 h exposure to celastrol (IC_{50} 2.10–9.01). C. Normal human epidermal keratinocytes treated as indicated (IC_{50} values >5 μM (8 h), 3.9 μM (16 h) and 3.70 μM (24 h)). D. Colony forming assays performed with OSCC cell lines treated with celastrol for 1 h (prior to washout) and allowed to grow until vehicle (DMSO) treated colonies reached 50 cells. The number of colonies in celastrol-treated wells is expressed as a percentage of the vehicle. For proliferation and colony forming assays error bars represent standard deviation of biological replicates. E. RT-qPCR

analysis of apoptotic genes in celastrol treated (6 h) OSCC cultures. For RT-qPCR 18 s ribosomal RNA was used as internal control and fold changes were determined using the delta delta CT method, error bars represent standard deviation of technical replicates.

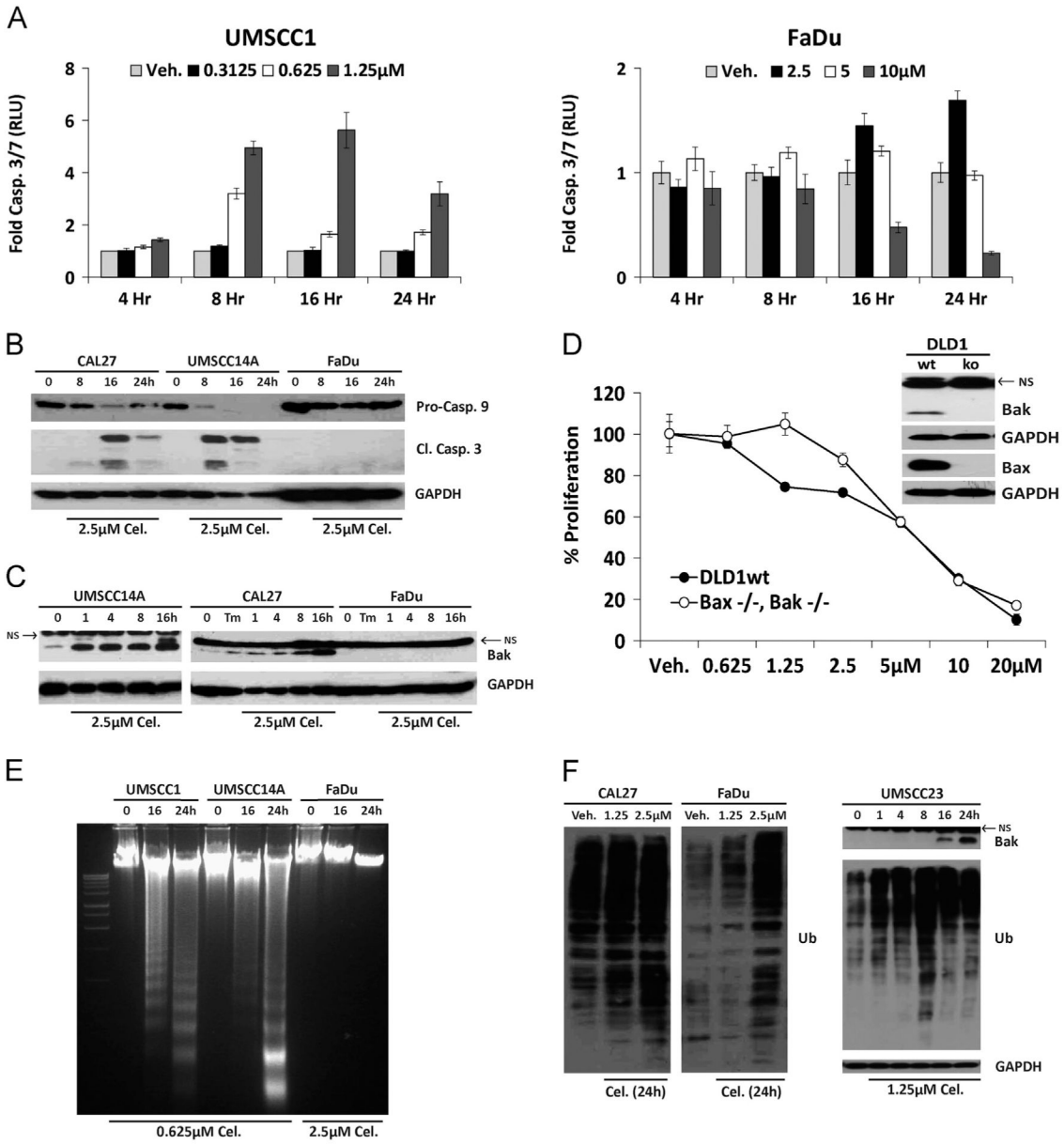

Fig. 3.

Celastrol induces apoptosis in OSCC cells. A. Luminescent caspase 3/7 assays performed with celastrol-sensitive (UMSCC1) and celastrol-resistant (FaDu) cells; error bars represent standard deviation of biological replicates. B. Immunoblot analysis of whole-cell lysates from celastrol-treated OSCC cells with polyclonal antibodies for Caspases-9 and -3. C. Immunoblot analysis of whole-cell lysates from OSCC cells with polyclonal antibody for Bak; NS=non-specific band present in all OSCC and DLD1 cells, including Bak−/−. D. Proliferation of wildtype or zinc finger deleted DLD1 $Bax^{-/-}$/$Bak^{-/-}$ colorectal adenocarcinoma cells treated for 24 h (Two-way ANOVA, *P* value <0.0001 for dose and interaction). E. Electrophoretic resolution of genomic DNA harvested from OSCC cultures to appreciate DNA laddering following celastrol exposure. F. Immunoblot analysis of ubiquitinated (total) proteins in whole cell lysates after 24 h (left); accumulation of

ubiquitinated proteins in UMSCC23 cells preceded Bak accumulation (right). For Immunoblot analysis, each membrane was stripped and re-probed with monoclonal GAPDH.

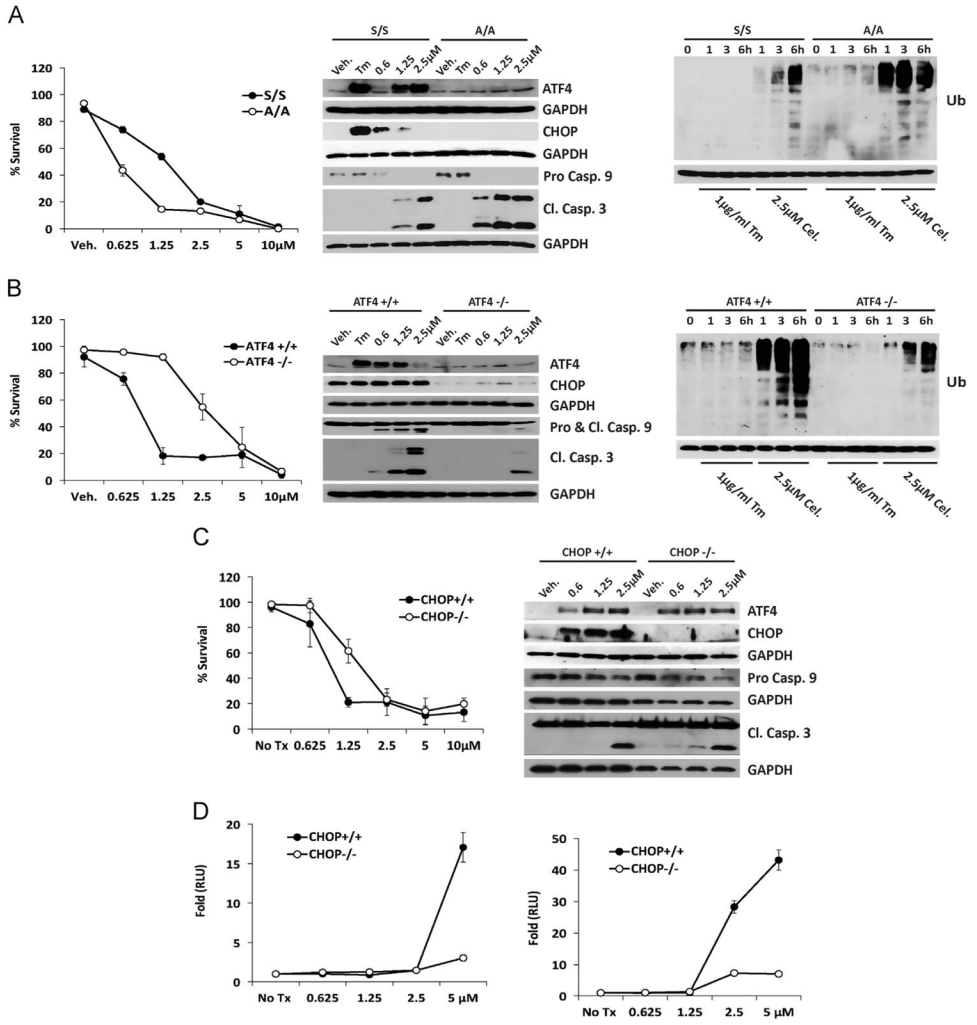

Fig. 4.

Intact UPR signaling is required for efficient celastrol-mediated apoptosis. A. Trypan blue exclusion assay performed with wildtype (S/S) and eIF2α ser51ala mutant (A/A) MEF treated with celastrol for 16 h (left) (Two-way ANOVA, *P* value <0.0001 for dose and 0.0060 for interaction); and immunoblot analysis of whole cell lysates with polyclonal antibodies for UPR and apoptotic protein transcripts (middle); and for Ubiquitin (Ub), as indicated. B. Trypan blue exclusion assay performed with wildtype and *Atf*4 −/− MEF (left) (Two-way ANOVA, *P* value <0.0001 for dose and for interaction); and immunoblot analysis of whole cell lysates with polyclonal antibodies for UPR and apoptotic protein transcripts (middle); and for Ubiquitin (Ub), as indicated. C. Trypan blue exclusion assay performed with wildtype and Chop −/− MEF treated with celastrol for 16 h (left) (Two-way ANOVA, *P* value <0.0001 for dose and interaction); and immunoblot analysis of whole cell lysates with polyclonal antibodies for UPR and apoptotic protein transcripts (right) D. Luminescent dose-response Caspase 3/7 enzymatic assay at four (left) and eight hours (right). All experiments were performed at least three times with triplicate samples; error bars represent standard deviation of biological replicates. For immunoblot analysis all membranes were stripped and re-probed with a monoclonal antibody for GAPDH.

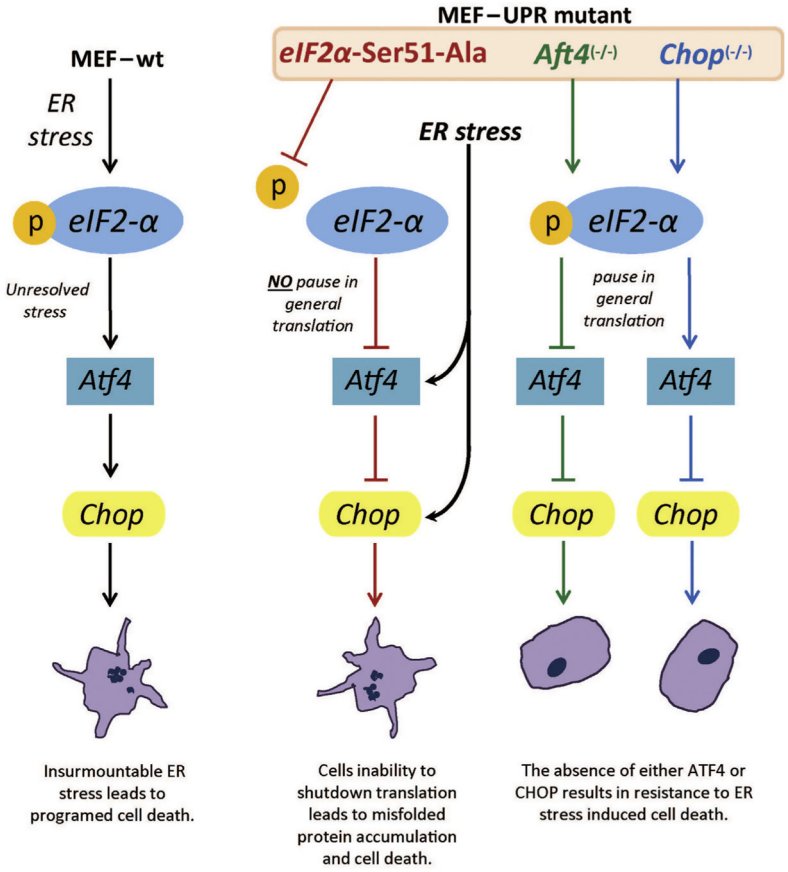

Fig. 5.

Model of cell death pathways in different UPR knockout murine embryonic fibroblasts. Death occurs if the eIF2α-mediated pause in translation does not occur or if CHOP accumulates following prolonged stress.